Available online at www.sciencedirect.com
ScienceDirect
Scripta Materialia 62 (2010) 361–364
Scripta MATERIALIA
www.elsevier.com/locate/scriptamat

A modified model for deformation via partial dislocations and stacking faults at the nanoscale

Pei Gu,[a] Bimal K. Kad[b] and Ming Dao[c,*]

[a] *MSC Software Corporation, 6050 Scripps St., San Diego, CA 92122, USA*
[b] *Department of Structural Engineering, University of California at San Diego, CA 92093-0085, USA*
[c] *Department of Materials Science and Engineering, Massachusetts Institute of Technology, Cambridge, MA 02139, USA*

Received 12 September 2009; revised 24 October 2009; accepted 27 October 2009
Available online 30 October 2009

The partial dislocation model for the deformation mechanism of nanocrystalline materials is extended to consider the influence of non-uniform dislocation extension. The non-uniform partial dislocation extension model is more consistent with experimental data than the original partial dislocation model. Additionally, the flow stress obtained from the non-uniform extension model is compared with that from the Hall–Petch relation.

Keywords: Partial dislocation; Stacking fault; Flow stress; Nanocrystalline material

Nanocrystalline metals with grain sizes in the nanometer-scale show appealing mechanical behaviors [1–3]. The Hall–Petch relation has been used to describe the variation of the flow stress or hardness with grain size down to the nanoscale [2,3]. The Hall–Petch relation [4,5] predicts that flow stress increases as grain size decreases. However, once the grain size becomes extremely small at the nanoscale (of the order of ~10 nm or less), the flow stress instead decreases with the grain size. This is known as grain size softening [6,7].

Recognizing the evidence of partial dislocations in nanocrystalline materials from experiments [8] and atomic-scale simulations [9], Asaro and coworkers [10,11] proposed a partial dislocation model for evaluating the shear stress required to emit intragranular partial dislocations and create stacking faults. In Asaro et al.'s model, the contribution to the required shear stress comes from the partial dislocation and stacking fault energies. In parallel, the partial dislocation mechanism was also investigated in Refs. [12,13] for related strengthening processes at the nanoscale. This intragranular emission of partial dislocation was incorporated into a three-dimensional constitutive methodology for numerical simulations of the mechanical behavior of nanostructures [14].

The partial dislocation model, also known as the stacking fault model, predicts higher mechanical strength than that measured from experiments [10]. One possible source of this discrepancy may arise from the fact that the model only considers that the emitted partial dislocation line is parallel to the original full dislocation line or the grain boundary, i.e., it assumes uniform extension. A more realistic case is that the propagating partial dislocation segment is no longer a straight line parallel to the grain boundary. In this paper, we propose a modified deformation mechanism through non-uniform partial dislocation extension. In other words, we extend the partial dislocation model developed in Ref. [10] to consider the influence of non-uniform partial dislocation extension.

As considered in Ref. [10], when the partial dislocation is emitted from the grain boundary, it creates two segments on the two lateral sides and the stacking fault, as shown in Figure 1a. The total energy consists of two portions: the energy in the two side segments and the energy associated with the propagating segment.

Consider a face-centered cubic metal whose primary slip system has the Burgers vector of dislocation $\mathbf{b} = a/2[1\,0\,\bar{1}]$, where a is the lattice parameter. The two Shockley partial dislocations are $\bar{\mathbf{b}} = a/6[2\,\bar{1}\,\bar{1}]$ and $\bar{\bar{\mathbf{b}}} = a/6[1\,1\,\bar{2}]$. When the partial dislocation $\mathbf{b}$ extends across the entire grain, the dislocation line is increased by $2d$ in length after creating two side segments, where d is the grain size. If the energy per unit length in the

* Corresponding author. Tel.: +1 (617) 253 2100. E-mail addresses: pei.gu@mscsoftware.com (P. Gu); bkad@ucsd.edu (B.K. Kad); mingdao@mit.edu (M. Dao).

1359-6462/$ - see front matter © 2009 Acta Materialia Inc. Published by Elsevier Ltd. All rights reserved.
doi:10.1016/j.scriptamat.2009.10.035

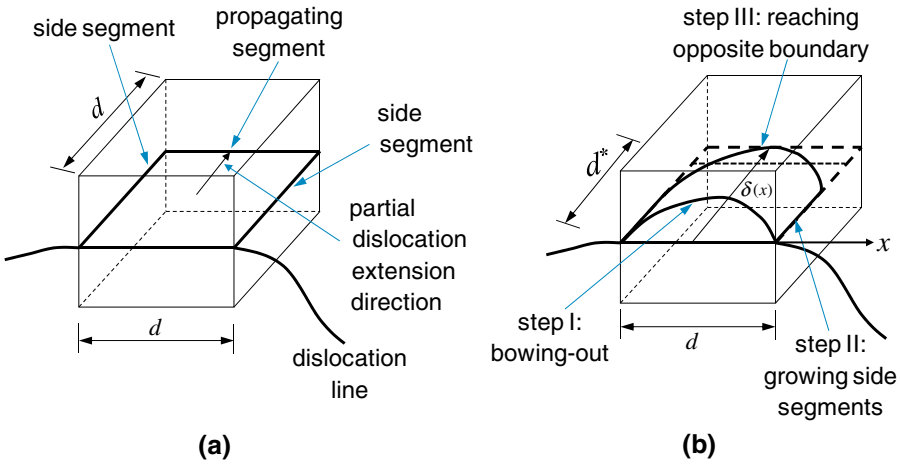

Figure 1. (a) Uniform partial dislocation extension. (b) Non-uniform partial dislocation extension.

side segments is taken as $1/2G\bar{b}^2$, where $\bar{b}$ is the magnitude of the Burgers vector of the partial dislocation and G is the shear modulus, the energy created in the two side segments is thus $1/2G\bar{b}^2 * 2d$. On the other hand, the work done by the resolved shear stress on the slip plane during the dislocation extension can be expressed as $(\tau_s\bar{b}_s + \tau_z\bar{b}_z)d^2$. Here, τ_s and τ_z are the components of the shear stress on the slip plane along the direction **s** and **z**, respectively; the $\bar{b}_s$ and $\bar{b}_z$ are the Burgers components in the direction **s** and **z**, respectively. The axis **s** is defined along the original dislocation line, the axis **m** is along the normal of the slip plane, and the axis **z** is perpendicular to the above two axes. Therefore, the shear stress required for the two side segments is

$$\tau \equiv \frac{\tau_s\bar{b}_s + \tau_z\bar{b}_z}{b} = G\frac{b}{3d}, \tag{1}$$

where b is the magnitude of **b**.

For the propagating portion of the partial dislocation, the energy per unit length E for moving the distance δ is given in Refs. [10,15] as:

$$E = -2E_{12}\ln\left(\frac{\delta}{r_0}\right) - (\tau_s\bar{b}_s + \tau_z\bar{b}_z)(\delta - r_0) + \Gamma(\delta - r_0), \tag{2}$$

where $E_{12} = G/(4\pi)\bar{b}_i\bar{\bar{b}}_i = 1/(24\pi)Gb^2$, Γ is the stacking fault energy, and r_0 is the radius of the dislocation core cut-off. Minimizing Eq. (2) with respect to δ, we obtain the equilibrium distance:

$$\delta = \frac{2E_{12}}{\Gamma - (\tau_s\bar{b}_s + \tau_z\bar{b}_z)}. \tag{3}$$

For extension across the grain, in the above expression we let $\delta = d$ and obtain the shear stress required for the propagating segment. Then, the obtained shear stress is combined with that given in Eq. (1) to obtain the required shear stress for the partial dislocation extension across the grain:

$$\frac{\tau}{G} = \frac{\Gamma}{Gb} + \gamma\frac{b}{d}. \tag{4}$$

In Eq. (4), $\gamma = 1/3 - 1/(12\pi)$. Expression (4) is the same as expression (7) in Ref. [10]. This shows the dependence of the flow stress on the grain size.

In deriving the required shear stress in Eq. (4), it is assumed that the propagating segment of the partial dislocation is parallel to the grain boundary. In other words, this means that the partial dislocation extension is uniform across the grain. It is likely that the dislocation extension is non-uniform. This is to say that, as systematically shown in Figure 1b, the propagating portion is not parallel to the grain boundary and is not a straight line. In the well-known Frank–Read source [16], the dislocation segment is pinned at the end points due to certain local barriers, and the applied shear force bows out the segment on the slip plane. Grain boundaries on the two lateral sides in Figure 1 can serve as such barriers to induce non-uniform dislocation emission into the grain. For example, as described in Ref. [16], an array of dislocations existing in low-angle grain boundaries on the lateral sides in Figure 1 can interact with the propagating dislocation and serve as the pinning points of the extending segments. In fact, detailed atomistic simulations, shown in Figure 4 of Ref. [9], have illustrated the formation, extension and approach to the opposite grain boundary of an intragranular, non-uniformly extending partial dislocation.

We shall consider non-uniform dislocation emission into the grain. Taking the following scenario for the dislocation extension, as shown in Figure 1b, the straight dislocation line is bowed out with pinned points on the two lateral sides of the grain in step I. When the curvature becomes sufficiently large, e.g., when further bowing-out with the two pinned points at the ends of the dislocation segment becomes impossible due to the lateral-side boundary constraint, further extension of the dislocation creates straight segments along the two lateral sides. In step II, the two side segments grow with further extension. In step III, together with the growth of the side segments, the extended partial dislocation finally reaches the opposite boundary of the grain. In order to capture the non-uniform extension inside the grain, we denote the extension distance of the propagating dislocation segment as $\delta(x)$, where x is the position along the originally straight dislocation line as shown in Figure 1b. We define the averaged extension distance inside the grain as:

$$d^* = \frac{1}{d}\int_0^d \delta(x)dx = \beta d. \tag{5}$$

Here, $\beta = 1/d^2 \int_0^d \delta(x)dx$. The extension parameter β, which is between 0 and 1, represents the influence of non-uniform partial dislocation extension.

Following similar steps that lead to the expression (4), we obtain the shear stress that is required for dislocation extension with the averaged extension distance d^* as:

$$\frac{\tau}{G} = \frac{\Gamma}{Gb} + \left(\frac{1}{3} - \frac{1}{12\pi\beta}\right)\frac{b}{d}. \tag{6}$$

The expression (6) is a linear relation with respect to d^{-1}, and the slope becomes negative for small values of β. The critical value is

$$\beta_c = \frac{1}{4\pi}. \tag{7}$$

For very small β, the second term in Eq. (6) is negative; in this case, it is dominant in the expression such that the value of the shear flow stress becomes negative. When this happens, the model does not predict the required shear stress due to insufficient dislocation extension. The lower bound for β given by Eq. (7) is independent of the material properties, whereas the upper bound for β is 1.

In addition to the intragranular emission of partial dislocations, another possible deformation mechanism is grain boundary sliding. Conrad and Narayan [17] proposed a model to account for grain boundary softening, i.e., the decrease of flow stress along with the grain size for sufficiently small grain. Expressions (6) and (7) suggest that the grain size softening may become the mechanism for the flow stress when the extension distance is less than that given in Eq. (7), $d^* < d/(4\pi) \approx 0.08d$.

The flow stress in Eq. (6) consists of a grain size independent term (the first term on the right-hand side) and a grain size dependent term (the second term on the right-hand side). From the definition in Eq. (5), it is seen that the extension parameter β is a function of the grain size d. By appropriately choosing β, it is possible to enforce the flow stress in Eq. (6) to follow the linear variation of $d^{-0.5}$ such that Eq. (6) agrees with the so-called Hall–Petch relation [4,5]. A Hall–Petch relation is expressed as:

$$\tau = k_0 + k_1 d^{-0.5}, \tag{8}$$

where k_0 and k_1 are the Hall–Petch constants.

Within the range that the Hall–Petch relation holds, let the second term on the right-hand side of Eq. (6) equal to the second term on the right-hand side of the Hall–Petch relation given in Eq. (8). We obtain the condition for Eq. (6) to follow the linear variation of $d^{-0.5}$:

$$\frac{1}{3} - \frac{1}{12\pi\beta} = A\sqrt{\frac{d}{b}}, \tag{9}$$

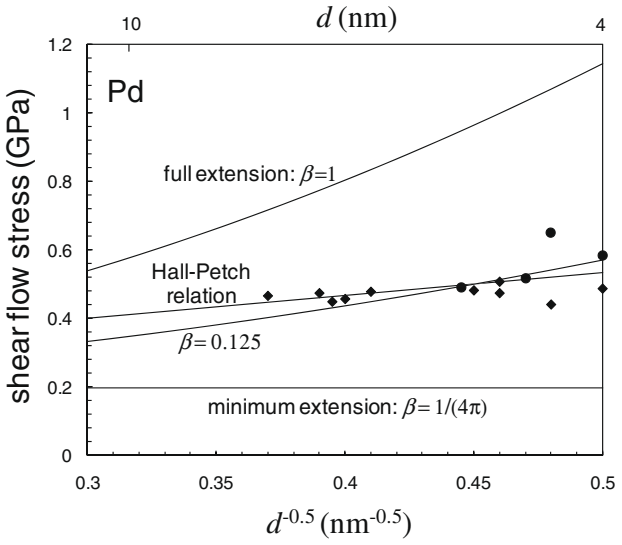

Figure 2. Comparison of non-uniform partial dislocation extension model with experimental data for Pd.

where $A = k_1/G/\sqrt{b}$ is a non-dimensional parameter. From Eq. (9), the extension parameter β that satisfies the Hall–Petch relation is given by:

$$\beta = \frac{1}{4\pi}\frac{1}{1 - 3A\sqrt{\frac{d}{b}}}. \tag{10}$$

The condition $1/(4\pi) \leqslant \beta \leqslant 1$, which was discussed previously, needs to be satisfied. For $\left(1 - 3A\sqrt{d/b}\right) \leqslant 1/(4\pi)$, we take $\beta = 1$. The expression (10) may be used to estimate the extension parameter β.

Now, the value of β can be estimated using the experimental data given in Refs. [3,18]. The two Hall–Petch constants for Pd are obtained from experimental data presented in Figure 2 in Ref. [18], by curve-fitting in the range $0.3 \leqslant d^{-0.5}(\mathrm{nm}^{-0.5}) \leqslant 0.5$. The two Hall–Petch constants for Cu are obtained from experimental data presented in Figure 1a in Ref. [3] and Figure 1 in Ref. [18], by curve-fitting in the range $0.1 \leqslant d^{-0.5}(\mathrm{nm}^{-0.5}) \leqslant 0.4$. The procedure to obtain β is as follows. First, let the grain size independent term in the Hall–Petch relation be equal to the grain size independent term in Eq. (6). This determines the value of Γ, for known b. Second, let the grain size dependent term in the Hall–Petch relation be equal to the grain size dependent term in Eq. (6). This determines β for known G, b, and d. Table 1 lists material properties and the values of β as well as the values of Γ, for Pd and Cu. The obtained values of Γ are within the ranges expected in the literature (e.g. [19]).

From Eq. (10) as well as the estimated values of β in Table 1, we see that the extension parameter increases along

Table 1. Material property and extension parameter β.

	G (GPa)	b (pm)	k_0 (MPa)	k_1 (MPa mm$^{0.5}$)	Γ (mJ m^{-2})	$d = 10$ nm	$d = 30$ nm
Pd	44	280	199	0.673	56	$\beta = 0.165$	$\beta = 0.777$
Cu	50	270	128	0.969	34	$\beta = 0.249$	$\beta = 1$

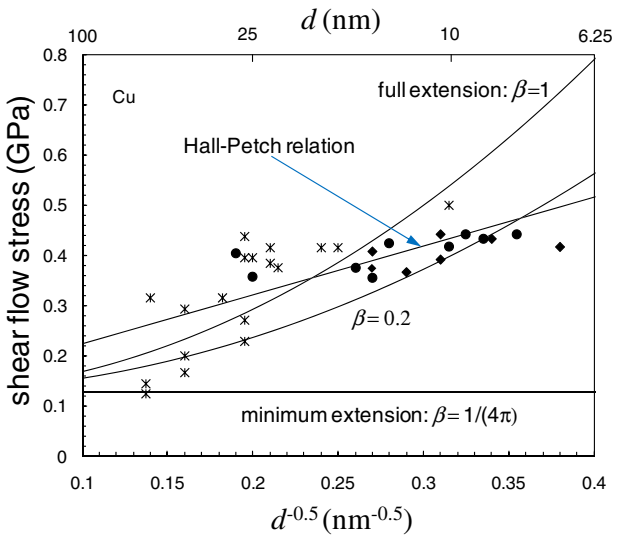

Figure 3. Comparison of non-uniform partial dislocation extension model with experimental data for Cu.

with the grain size. This may be understood from the perspective that the propagating segments are likely to retain smaller curvatures in larger grains than smaller grains.

The variation of the shear flow stress with $d^{-0.5}$ for the cases of representative β values and the Hall–Petch relation is plotted in Figure 2 for Pd. The shear flow stress for these extension parameters is plotted in Figure 3 for Cu. Expressions (6) and (8), as well as the material properties in Table 1, are used to make these two figures. The circle-shape and diamond-shape points shown in Figures 2 and 3 are the measured data from Figures 1 and 2 in Ref. [18], where circle-shape points and diamond-shape points are from two different samples. The star-shape points in Figure 3 are measured data from Figure 1a in Ref. [3]. In Refs. [3] and [18], experimental data were presented in terms of Vickers hardness. The hardness data are divided by 6 to convert to the shear flow stresses in Figures 2 and 3 [10]. The curves for the full extension case, $\beta = 1$, represent the original model proposed in Refs. [10,11]. The curves for $\beta = 1/(4\pi)$ and $\beta = 1$ are the lower bound and upper bound of the shear flow stress, respectively, for a sufficiently small grain size. It is seen that the original model proposed in Refs. [10,11] considerably overestimates the flow stress for smaller grain sizes on the right side of the two figures. In other words, the modified model for non-uniform partial dislocation extension may be used to better estimate the flow stress of a nanocrystalline material.

For known extension parameter β and grain size d, the extension distance $\delta(x)$ along the dislocation line can be obtained by solving the integral equation given in Eq. (5). In the continuum theory of dislocations, the solution for the extension distance is not unique. Atomic-scale simulations may be used to analyze intragranular dislocations and stacking faults in more detail (i.e. [9]).

In summary, the partial dislocation model for the deformation mechanism of nanocrystalline materials is extended to consider the non-uniform partial dislocation extension. The flow stresses obtained from the non-uniform partial dislocation model are consistent with experimental data. The non-uniform partial dislocation model is compared with the Hall–Petch relation. Finally, we note that rate sensitivity can be included in the non-uniform partial dislocation model using the constitutive approach discussed in Ref. [14].

M.D. acknowledges support from the Office of Naval Research Grant N00014-08-WR-2-0227 on "Surface Engineering and Mechanisms of Damage Evolution at Tribologically Active Surfaces," and from the Infectious Disease Interdisciplinary Research Group of the Singapore-MIT Alliance for Research and Technology (SMART).

[1] H. Gleiter, Prog. Mater. Sci. 33 (1989) 223.
[2] M.A. Meyers, A. Mishra, D.J. Benson, Prog. Mater. Sci. 51 (2006) 427.
[3] M. Dao, L. Lu, R.J. Asaro, J.T.M. De Hosson, E. Ma, Acta Mater. 55 (2007) 4041.
[4] E.O. Hall, Proc. Phys. Soc. Lond. Sect. B 64 (1951) 747.
[5] N.J. Petch, J. Iron Steel Inst. 174 (1953) 25.
[6] A.H. Chokshi, A. Rosen, J. Karch, H. Gleiter, Scripta Mater. 23 (1989) 1679.
[7] K. Lu, M.L. Sui, Scripta Mater. 28 (1993) 1465.
[8] L. Lu, Y. Shen, X. Chen, L. Qian, K. Lu, Science 304 (2004) 422.
[9] H. Van Swygenhoven, M. Spaczer, A. Caro, Acta Mater. 47 (1999) 3117.
[10] R.J. Asaro, P. Krysl, B. Kad, Philos. Mag. Lett. 83 (2003) 733.
[11] R.J. Asaro, S. Suresh, Acta Mater. 53 (2005) 3369.
[12] Y.T. Zhu, X.Z. Liao, S.G. Srinivasan, Y.H. Zhao, M.I. Baskes, F. Zhou, E.J. Lavernia, Appl. Phys. Lett. 85 (2004) 5049.
[13] Y.T. Zhu, X.Z. Liao, S.G. Srinivasan, E.J. Lavernia, J. Appl. Phys. 98 (2005) 034319.
[14] B. Zhu, R.J. Asaro, P. Krysl, R. Bailey, Acta Mater. 53 (2005) 4825.
[15] R.J. Asaro, J.R. Rice, J. Mech. Phys. Solids 25 (1977) 309.
[16] D. Hull, D.J. Bacon, Introduction to Dislocations, fourth ed., Butterworth, Heinemann, Oxford, 2001.
[17] H. Conrad, J. Narayan, Scripta Mater. 42 (2000) 1025.
[18] G.E. Fougere, J.R. Weertman, R.W. Siegel, S. Kim, Scripta Mater. 26 (1992) 1879.
[19] J.P. Hirth, J. Lothe, Theory of Dislocations, second ed., Wiley, New York, 1982.